Overview of recent advancements in IFMIF-DONES neutronics activities

Y. Qiu [a,*], M. Ansorge [b], I. Álvarez [g], K. Ambrožič [e], T. Berry [c], B. Bieńkowska [d], H. Chohan [c], A. Čufar [e], D. Dworak [f], T. Dezsi [s], T. Eade [c], J. García [g,a], D. Jimenez-Rey [h], I. Lengar [e], A. J. Lopez-Revelles [i], V. Lopez [i], E. Mendoza [h], F. Mota [h], M.J. Martinez-Echevarria [g], F. Ogando [i], J. Park [a], T. Piotrowski [j], A. Serikov [a], G. Stankunas [k], A. Tidikas [k], G. Tracz [f], G. Žerovnik [e], F. Arbeiter [a], F. Arranz [h], S. Becerril [l], P. Cara [m], D. Bernardi [n], J. Castellanos [o], J. Gutiérrez [p], A. Ibarra [h,l], W. Królas [f], J. Maestre [g,l], F. Martín-Fuertes [h], J.C. Marugán [p], G. Micciché [n], J. Martínez-Serrano [q], F.S. Nitti [n], I. Podadera [h,l], U. Wiącek [f], U. Fischer [r]

[a] Karlsruhe Institute of Technology, Karlsruhe (KIT), Federal Republic of Germany
[b] Nuclear Physics Institute of the Czech Academy of Sciences, Řež 250 68, Czech Republic
[c] UKAEA, Culham Science Centre, Abingdon OX14 3DB, UK
[d] Institute for Plasma Physics and Laser Microfusion (IPPLM), 23 Hery Str., Warsaw 01-497, Poland
[e] Reactor Physics Department, Jožef Stefan Institute, Jamova Cesta 39, Ljubljana SI-1000, Slovenia
[f] Institute of Nuclear Physics Polish Academy of Sciences (IFJ PAN), ul. Radzikowskiego 152, Cracow 31-342, Poland
[g] Universidad de Granada, C/Gran Vía de Colón 48, Granada 18010, Spain
[h] Centro de Investigaciones Energética Medioambientales y Tecnológicas (CIEMAT), Madrid, Spain
[i] Universidad Nacional de Educación a Distancia (UNED), Madrid, Spain
[j] Warsaw University of Technology, Al. Armii Ludowej 16, Warsaw 00-637, Poland
[k] Lithuanian Energy Institute, Laboratory of Nuclear Installation Safety, Breslaujos str, Kaunas 44403, Lithuania
[l] Consorcio IFMIF-DONES España, C/Gran Vía de Colón 48, Granada 18010, Spain
[m] Fusion for Energy, Garching, Federal Republic of Germany
[n] ENEA, Brasimone, Camugnano (BO) 40032, Italy
[o] INAIA, Universidad de Castilla la Mancha, Toledo, Spain
[p] Empresarios Agrupados International (EAI), Madrid, Spain
[q] Universidad de Málaga, Málaga, Spain
[r] Independent researcher, Karlsruhe, Federal Republic of Germany
[s] C3D Engineering Ltd, Budapest 1106, Hungary

ARTICLE INFO

Recent advancements in the neutronics activities of the IFMIF-DONES project, developed within the EUROfusion framework, are presented. These include updates to radiation dose maps during commissioning and normal operation of the accelerator systems; material irradiation analyses and shielding optimization of the test systems; activation inventories of ^{7}Be, ^{3}H, and activated corrosion products in the Li systems; shutdown dose analyses of transportation and storage of radioactive waste, cooling water and atmosphere gas activations, skyshine to the public, etc. The development of simulation tools, nuclear data evaluation, and nuclear experiments for the specific needs of DONES neutronics are highlighted, as well as the nuclear analysis handbook and database. Several challenges for future development are also discussed to ensure the provision of high-quality nuclear analyses.

1. Introduction

IFMIF-DONES (International Fusion Materials Irradiation Facility – Demo Oriented NEutron Source, abbreviated as DONES [1,2]) is a one-of-a-kind accelerator-based fusion prototypic neutron irradiation facility under construction in Granada, Spain. It is being developed by the DONES Program governed by the IFMIF-DONES España consortium, with participation from several EU countries, UK and Japan. The primary mission of DONES is to provide crucial materials data for the design, construction, and safe operation of the DEMO fusion power

---

plant, as well as data for materials modeling. This will be achieved by providing high-intensity neutron irradiation equivalent to that at the first wall of a fusion reactor. DONES utilizes a high-current deuteron accelerator operating in Continuous Wave (CW) mode at 40 MeV and 125 mA to impinge the deuteron particles into a high-speed (15 m/s) flowing Li curtain. This produces high-intensity neutrons with energies up to 55 MeV and peak fluxes of 10^{15} n/cm^2/s through d-Li stripping reactions. The neutrons will be used to irradiate material samples housed in test modules behind the target, and perform complementary experiments [3].

IFMIF-DONES [1] consists of the accelerator systems (AS) which produce, accelerate, shape and transport the deuteron beam to the target; the lithium systems (LS) for circulating, cooling and purifying the liquid-lithium through the target; the test systems (TS) related to the irradiation process, irradiation modules and their management; buildings and plant systems (BPS) that provide hosting and auxiliaries; and also the central instrumentation and control systems (CICS) which ensure the control and safe operation of the plant. Fig. 1 is a schematic view of the plant configuration.

Significant progress has been made recently in DONES neutronics activities within the EUROfusion Framework Programme FP9. Nuclear analyses have been conducted comprehensively on beam-on and beam-off radiation doses, nuclear responses, activation inventories, and shielding optimizations. These analyses have systematically considered the radiation source terms, including neutrons and photons produced from deuteron beam losses, beam depositions in the beam scrapers, collimators, beam dump and, most importantly, from the Li target. They have also considered the activation produced by deuterons and neutrons impinging on the structures, lithium, cooling water, corrosion products, air, and atmospheric gases. These nuclear analyses provide crucial data for the design optimizations, licensing, construction, commissioning, and operation of DONES systems, as well as inputs for remote handling, logistics and maintenance, safety, and beyond.

This paper provides an overview of recent DONES neutronics activities and their progress, by first presenting in Section 2 the simulation tools and data adopted and developed in the project, and successively the design and analyses carried out across several systems, which are presented in Section 3. Then Section 4 will discuss recent ongoing nuclear data and experiments, as well as important practices for managing the data. Finally, Section 5 will provide a summary and discussions on future advancements.

2. Simulation methods, tools and data

Tools and data are essential for neutronics activities. Deuteron transport codes and special tools and data, such as MCUNED [4] and McDeLicious [5], which are based on the Monte Carlo (MC) transport
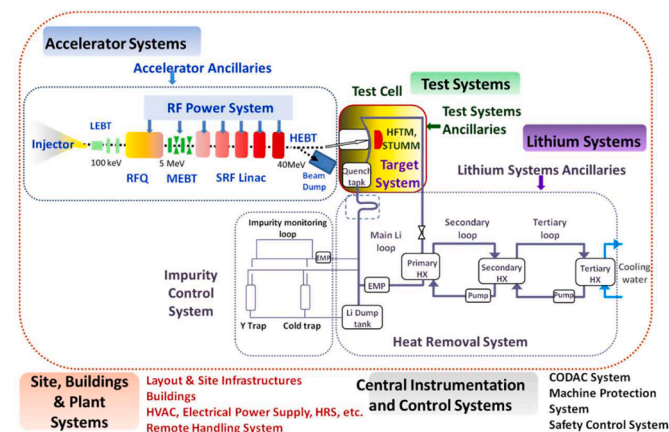
code MCNP [6], are heavily relied upon for DONES applications. MCUNED has been the reference code for the simulation of DONES accelerator systems since the project began. It is an extension of MCNP that provides capabilities for simulating deuteron transport with specially corrected neutron angular distribution from the deuteron breakup reaction. It also provides a dedicated variance reduction technique for deuteron-induced neutron production to increase the secondary neutron sampling efficiency. For the d-Li reactions in the target, McDeLicious provides the capability to simulate the generation of neutrons and photons based on the use of evaluated d + ^{6,7}Li cross-sections FZK-2005 [7]. Recent comparisons [8] on d-Li nuclear data suggest that the d-Li data from JENDL/DEU-2020 (currently integrated into JENDL-5 [9]) are also suitable for DONES neutronic simulation. In addition to the full-fledged deuteron MC simulation codes, a recently developed tool, srcUNED-Ac [10], which is an MCNP source module, allows reproducing secondary neutrons and gammas from deuteron interaction with materials along the accelerator with a precomputed double-differential spectra, without the need to perform deuteron transport simulation. Some alternative codes for the DONES-like accelerator neutron source simulation, such as OpenMC, have also been studied [11], providing open-source alternatives for research training.

DONES has similar geometric complexities as other fusion facilities, thus common CAD-to-MC modeling tools such as McCad [12], SuperMC [13] and MCNP geometry toolkits Numjuggler [14] are accepted. Additionally, the recently developed Python- and FreeCAD-based GEOUNED [15] code provides robust and easy-to-use geometry modeling, with good demonstrations in recent accelerator system modeling. Activation inventory tools such as FISPACT [16] and ACAB [17] are suitable for DONES simulations in principle, with proper selection of nuclear data and group structures, such as the 211-group Vitamin-J+ and 709-group CCFE structures [18], which provide energy bins covering 55 MeV. For Shutdown Dose Rate (SDR) simulation, rigorous two-step-based tools such as MCR2S [19], R2Smesh [20], and R2SUNED [21], which have been validated for neutron activation in fusion applications, are accepted for DONES application when suitable activation libraries are called. Special attention must be paid to deuteron activation, as 40 MeV deuterons result in penetration depths of a few millimeters. Therefore, direct one-step (D1S) SDR tools, particularly D1SUNED [22], which have the capability to simulate light ion-induced activation, are recommended. In addition, tools for liquid activation and source modeling, e.g. Actiflow [23] and CAD2CDGS [24] have been demonstrated with good applicability for radiation analysis of activated water and Li.

Variance reduction is essential for neutron and photon shielding calculations in DONES, which has several meters of concrete shielding with many penetrations. The ADVANTG [25] weight-window mesh (WWM) generation tool uses a deterministic solver to compute global priori neutron flux for global and local WWMs. Sometimes it shows deficiencies in DONES simulations due to strong streaming through the penetrations. The OTF-GVR [26] WWM tool, which uses an MC-based flux-WWM iterative process and an algorithm for controlling over-splitting particles, shows good performance in DONES shielding analysis.

One outstanding need of DONES neutronics is high-quality deuteron transport and activation libraries. TENDL libraries [27], which are based on the physics model implemented in the TALYS code [28], have been used as the current reference deuteron libraries. However, they have known deficiencies in the reaction models for deuterons [29]. These models have been consistently improved in the TALYS code [30] for the involved reaction mechanisms, including breakup, pick-up, pre-equilibrium, and evaporation processes. However, these improvements still have to be fully included in the latest TENDL-2021 deuteron libraries. The recent release of JENDL-5 has provided several important target materials (^{6,7}Li, ^{9}Be, and ^{12,13}C) [31], as well as important elements for accelerator component materials (^{27}Al, ^{63,65}Cu, and ^{93}Nb). Ongoing reviews of JENDL-5, such as the review of the ^{63,65}Cu data [32], show

Fig. 1. Schematic view of DONES systems [1].

clear improvements in the deuteron libraries of JENDL-5 compared to those of TENDL-2021. FENDL-3.1d [33] is the current reference neutron cross section library. It is expected to be replaced soon by the newly released FENDL-3.2 [34] after sufficient tests with benchmarks and verification comparisons on full-scale DONES simulations. Apart from general neutron cross sections, special displacement cross sections [35] based on the NRT (Norgett-Robinson-Torrens) and arc-dpa models for Eurofer steel, stainless steel (SS), and other single elements were used in both the DONES project and the European DEMO project for consistency. All these tools and data are important foundations for the nuclear analyses presented in the following sections.

3. Neutronics activities in DONES systems

3.1. Neutronics activities in accelerator systems

DONES accelerator systems (AS) [36] shown in Fig. 2 deliver a properly shaped 125 mA, 40 MeV deuteron beam using a 175 MHz continuous-wave (CW) linear accelerator. Its main components are an injector made of an ion source at 100 keV energy, coupled with a low-energy transport (LEBT) line. The beam is then further bunched and accelerated by the radio frequency quadrupole (RFQ) up to 5 MeV, transported through the Medium Energy Beam Transport (MEBT) line and then accelerated by the Superconducting Radio Frequency LINear ACcelerator (SRF LINAC) to the final energy of 40 MeV. In the High Energy Beam Transport (HEBT) line, the beam is shaped to a quasi-rectangular beam footprint by magnets and scrapers, guided to the High Power Beam Dump (HPBD) during the commissioning phase, and transported to the Li target during normal operation.

The main radiological source terms in the AS are generated by beam depositions along the accelerator lines due to distributed beam losses along the vacuum tube and localized ones in collimation devices. Realistic distributed beam losses of up to 1000 W/m are expected in low-energy part of the RFQ, while a 1 W/m beam loss assumption was adopted for computing the radiation from MEBT, SRF and HEBT supported by beam dynamics simulations. These deuterons interact with the aluminium and stainless steel in the MEBT, SRF and HEBT beam pipe, with copper in the RFQ, and with niobium in the SRF LINAC cavities. One of the main contributions to the residual doses is ^{56}Co ($T_{1/2} = 77.2$ d), which is produced from the reaction ^{56}Fe (d,2n) and emits strong gammas during a long maintenance period. Efforts were therefore made to change beam-facing materials from stainless steel to aluminium [37], which produces the relatively short-lived ^{24}Na ($T_{1/2} = 14.9$ h). During normal operation, the scrapers used for collimating the beam receive a 0.3 kW beam deposition at 5 MeV in each MEBT copper scraper, and 2.4 kW and 3.2 kW in the first and second HEBT CuCrZr scrapers at the beam energy of 40 MeV.

Nuclear analyses are performed for both the commissioning stages and the normal operation of the accelerator, which operates in four phases [38]. During Phase 1 of injector commissioning at 140 mA continuous wave (CW) mode, neutron emissions from deuteron interaction with the lower power beam dump copper cone are few because the 100 keV deuteron energy is below the threshold of most of the d-Cu nuclear reactions. Instead, neutrons are mostly emitted from

deuteron-deuteron fusion reactions due to the implanted deuteron on the cone, and are expected to be 1.36×10^8 n/s under 140 mA CW operation according to the measurement [39]. Phase 2 commissioning of the RFQ, MEBT, and HPBD is planned to operate the machine with a 20 % duty cycle (DC) at a beam energy of 5 MeV for a maximum integrated beam time of two months. This produces residual biological doses of 100 μSv/h near the MEBT and the entrance of the HPBD, and above 10 μSv/h in the meters around the accelerator after 1 h of cooling (see Fig. 3) [40]. As ^{64}Cu dominates in the deuteron-induced HPBD activation, the doses are expected to reduce by >70 % after 1 day of cooling. Phase 3 commissioning on the superconducting radio frequency (SRF) operates the accelerator at 1 % DC at 40 MeV, resulting in a 50 kW beam deposition in the HPBD. The residual dose in Fig. 4 after 4 years of conservative commissioning phase and 1 h cooling is higher than 1 mSv/h surrounding the HPBD, due to decay gammas from ^{56}Mn ($T_{1/2} = 2.57$ h) and ^{64}Cu ($T_{1/2} = 12.7$ h) in the first several hours of cooling, and then ^{58}Co ($T_{1/2} = 70.8$ d), ^{65}Zn ($T_{1/2} = 244$ d), and ^{60}Co ($T_{1/2} = 5.27$ y), which result in slow decreases of residual dose from 1 day to weeks.

During normal operation in continuous wave (CW) mode, the radiation (beam-on dose map in Fig. 5 and beam-off dose map in Fig. 6) inside the accelerator vault is mainly contributed by beam deposition at the high energy beam transport (HEBT) scraper, beam losses along the HEBT, and back-scattered neutrons from the test cell (TC). The neutron production in the first HEBT scraper is as high as 10^{13} n/s, resulting in a high residual dose of 10 mSv/h after 1 h cooling near the scraper shielding. This dose is dominated by gammas from ^{63}Zn ($T_{1/2} = 38.3$ min), ^{64}Cu, and ^{65}Zn produced from Cu(d,x) reactions. Depending on the workloads during maintenance (still in the definition phase) and dose rates, hands-on maintenance is assumed free for areas below 10 μSv/h, and remote handling is directly required for areas above 100 mSv/h. The areas with moderate doses of 10 μSv/h–100 mSv/h are subjected to an ongoing ALARA (As Low As Reasonably Achievable) approach to reduce occupational radiation exposures.

Water is used for cooling the first HEBT scraper, while helium is used for the second scraper to avoid the possible entrance of water into the beam pipe, which is a safety barrier, so as to prevent water reaction with Li. Water activation in the HEBT scraper is not a major concern due to the short water activation time (in a few seconds), short half-life of the radioisotopes, and the long distance of more than 12 m to the exit of the AS vault. The specific activity is at the level of 10^5 Bq/kg, dominated by ^{16}N ($T_{1/2} = 7.1$ s) from the ^{16}O(n,p) reaction and ^{15}O ($T_{1/2} = 122$ s) from the ^{16}O(n,2n) reaction, a threshold reaction at 16 MeV. Activated Corrosion Products (ACP) due to water corrosion on CuCrZr scraper blades are less significant due to the low corrosion rate at the low operation temperature of 20–30 °C [41].

Air in the AS vault and argon gas inside the Target Interface Room (TIR) will be activated by neutrons, producing mainly ^{41}Ar ($T_{1/2} = 1.8$ h) from the ^{40}Ar(n,p) reaction. With the current design of the Heating, Ventilation, and Air Conditioning (HVAC) system, the level of ^{41}Ar in the AS vault reaches 10^7 Bq. The high level of activity in the TIR, a forbidden-access cell, 8.2×10^{10} Bq, requires room isolation and a decay time when changing to beam-off mode to reduce contamination. The
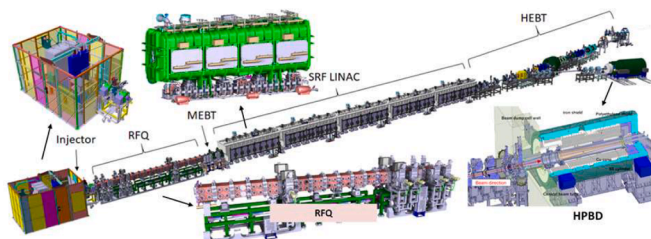

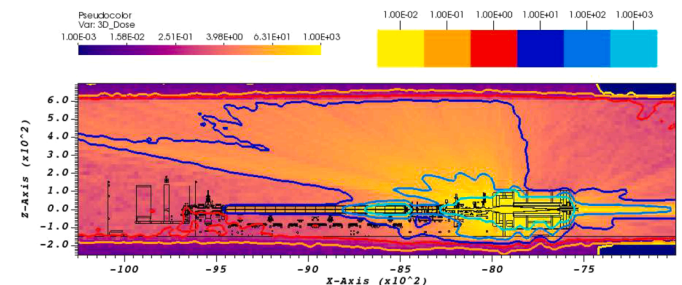**Fig. 2.** Schematic view of the DONES accelerator and its main components.

Fig. 3. Total residual dose rate (μSv/h) in Phase 2 commissioning accelerator after a decay time of 1 h.

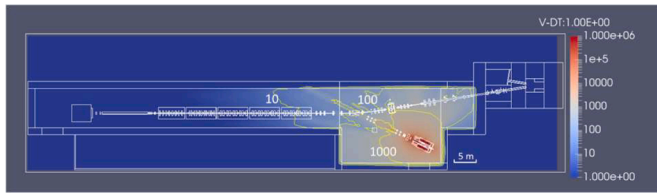**Fig. 4.** Total residual dose rate (μSv/h) 1 h after shutdown in Phase 3 commissioning.
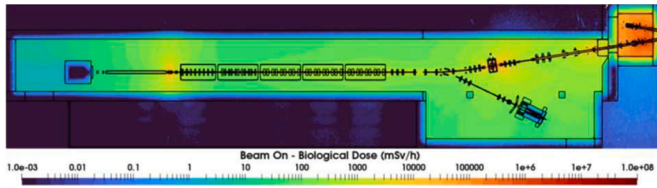

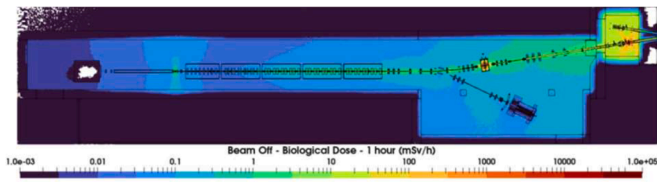**Fig. 5.** Biological dose (mSv/h) during operation of the accelerator in the AS room.

Fig. 6. Biological dose (mSv/h) at 1 h of cooling time in the AS room.

activation of gases (argon, D_2) inside the beam pipe is dominated by deuteron activation of argon, resulting in a total activity rate of 3.0×10^4 Bq/s contributed by several short-lived isotopes ^{40}Cl ^{39}Cl, ^{38}Cl, ^{38}K, ^{37}S, and ^{41}Ar.

3.2. Neutronics activities in test systems

The Test Cell (TC), which houses the Target Assembly (TA) and the
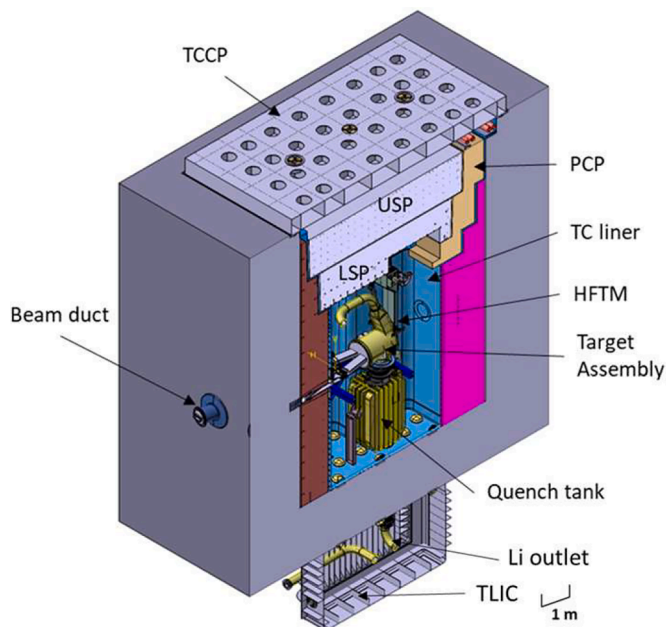

Fig. 7. Geometry of the TC and internal components.

High Flux Test Module (HFTM), is shown in Fig. 7. It has a massive shielding structure consisting of a stainless steel liner for atmosphere and safety confinement, and Removable Biological Shielding Blocks (RBSBs) cladded with 5 cm steel liners, filled with heavy concrete, and cooled by water. Outside the RBSBs is a concrete bucket that provides structural support and additional shielding for the surrounding areas and the floor. The upper part of the TC is shielded with a helium-cooled Lower Shielding Plug (LSP) and an Upper Shielding Plug (USP) filled with heavy concrete. The LSP and USP are covered by a Test Cell Cover Plate (TCCP) that provides atmospheric sealing and additional shielding. The helium coolant and cables for the HFTM and other inner components go through the Pipe and Cabling Plugs (PCPs), which have a zig-zag shape to mitigate radiation streaming. The deuteron beam is transported through the 27×12 cm^2 beam duct and impinges on the Li curtain with a quasi-rectangular footprint. The neutrons irradiate the steel samples (mainly EUROFER for the first test module that will be irradiated during the IFMIF-DONES operation phase [42]) housed in the HFTM under controlled temperatures.

As the main source of radiation, the d-Li reaction produces neutrons through Li(d,xn) stripping reactions, with a total yield of $\sim6.8 \times 10^{16}$ n/s (calculated using McDeLicious with FZK-2005 data [7]) and a broad peak around 14 MeV emitted at the forward angle. The neutron and photon flux in Fig. 8 shows a neutron flux of 1–5×10^{14} cm^{-2}s^{-1} and a photon flux of 5×10^{13} - 2×10^{14} cm^{-2}s^{-1} in the center four columns of the HFTM capsules. The deuteron beam footprint has a flexibility between the nominal size of 20×5 cm^2 and the reduced size of 10×5 cm^2 to optimize the irradiation intensity and gradient. The reference beam footprint originating from the IFMIF/EVEDA [5] has been recently validated through beam dynamics simulations, proposing new alternative profiles (Fig. 9) that have a similar shape but a better DPA-volume performance at a high damage rate as shown in Fig. 10. According to the top-level requirement, the volume above 16.7 dpa/year should be > 100 cm^3, and the volume between 8 and 12 dpa/year should be > 300 cm^3. The values in Fig. 10 show that these requirements are met, although the availability of the facility could reduce the expected yearly damage dose by 25 % [43].

Most of the 5 MW deuteron beam energy is deposited in the high-speed Li flow, with a peak value under the nominal footprint of over 110 kW/cm^3 at the Bragg peak position, which is about 20 mm deep. The remaining energy is spread over neutrons and gamma rays to the target assembly (TA, ~6.9 kW excluding Li), High Flux Test Module (HFTM, ~17 kW), steel liner (~15 kW), and Removable Biological Shielding Blocks (RBSB, ~77 kW). These values have slightly changed from the previous calculation [44] due to the design evolution.

The DPA calculation presented in Fig. 10 is estimated over the continuous volume of the HFTM, where the sample regions are filled with a homogeneous mixture of EUROFER and sodium. The simulation of a typical payload of small specimen test technology (SSTT) samples obtains similar DPA-volume curves over the sample volume (shown in Fig. 11), thus justifying the approximation of using the homogeneous
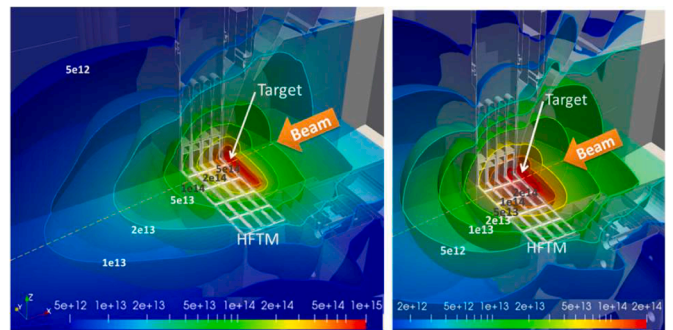

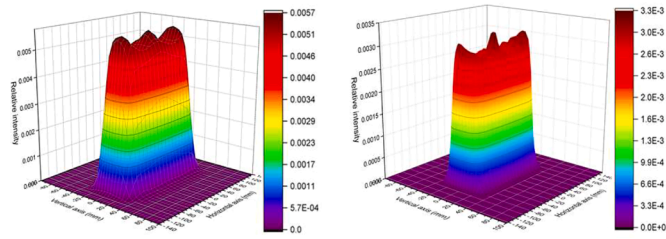**Fig. 8.** Distributions of the neutron (left) and photon (right) flux density in the TA and HFTM.

Fig. 9. The IFMIF/EVEDA 20 × 5 cm^2 beam profile (left) and the validated profile with a center-peak (right).
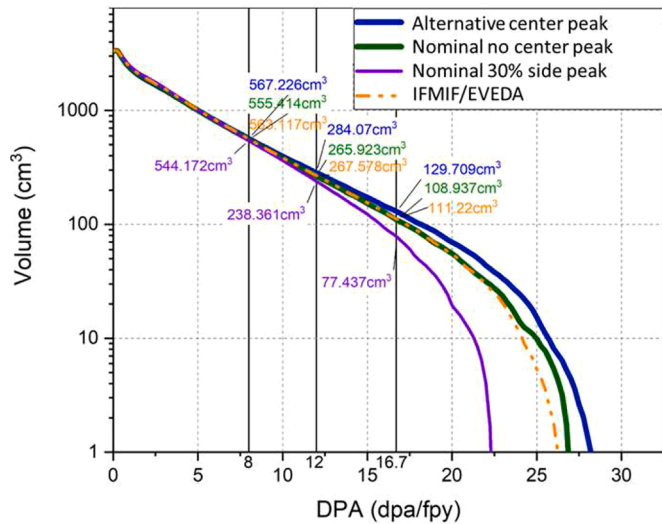

Fig. 10. The DPA-volume curve for different beam profiles over the continuous volume of HFTM. "IFMIF-EVEDA" is the previous reference; "Nominal 30 % side peak" has a high side peak to reduce DPA gradient; "nominal no center peak" has a similar beam size as IFMIF/EVEDA profile; and "Alternative center peak" has IFMIF/EVEDA profile size with a center peak.
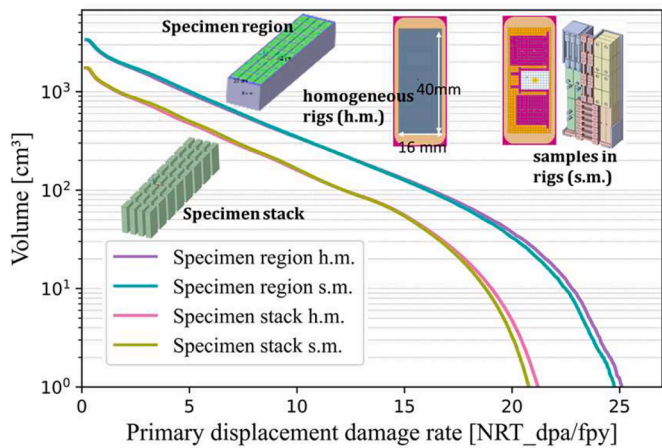

Fig. 11. DPA-volume of HFTM with homogenous sample mixture and detailed SSTT payload.

sample model. In addition to the samples in the HFTM, the TA back-plate can also be considered for potential EUROFER samples, which would provide an additional 100 cm^3 of irradiated material volume with high damage doses [45].

The neutron dose rate shown in Fig. 12 decreases from 10^{12} μSv/h inside the TC to a few μSv/h outside, a reduction of nearly 11 orders of magnitude. Neutron radiation contributes to the majority of the beam-
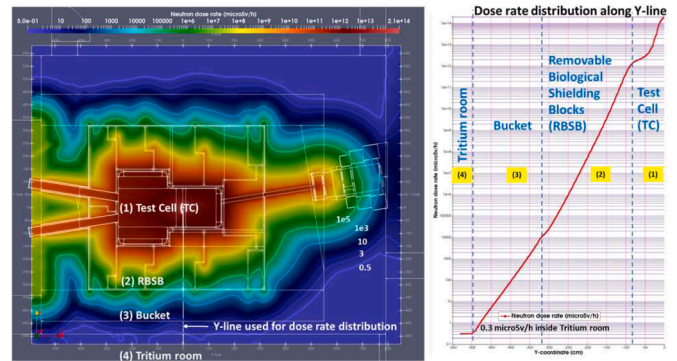

Fig. 12. Neutron dose rate (μSv/h) for the TC at horizontal cut-view.

on biological doses, with prompt gamma radiation contributing less than 10 %. However, prompt gamma radiation contributes more than 80 % of the total nuclear heating in the TC liner and bio-shield [44], due to the large Fe(n,g) contribution from neutrons interacting with the steel and heavy concrete. Neutron streaming is clearly visible through the 40 mm RBSB gaps, but does not significantly impact shielding in horizontal directions, even though the heavy concrete for the bucket is replaced by ordinary concrete. However, neutrons streaming through the vertical RBSB gaps with dogleg structures are strong in the room above the TC. Shielding optimizations such as filling the TCCP with polyethylene help to reduce the doses to the allowable level.

Water activation is a concern because of the high flow rate of around 23 L/s for the RBSBs and 0.9 L/s for the liner through long and complex cooling pipes. Unlike ^{16}N, which will quickly reach equilibrium, ^{15}O will accumulate along the flow path and therefore require a well-shielded decay volume before the water enters the heat exchanger. The expected specific activity at the exit of the cooling pipe is at the level of ~2 × 10^9 Bq/kg. Helium is the atmosphere gas for the inner TC, thus will not cause any activation. However, the air in the gaps between the liner and the RBSBs is highly activated at the level of 1.0 × 10^{11} Bq after 1-year operation assuming no air circulation. The activity decreases to ~10 % after 1-day cooling due to short-lived ^{41}Ar, but the residual activities will increase with more years of operations due to the long-lived isotopes ^{3}H ($T_{1/2}$ = 12.3 y), ^{14}C ($T_{1/2}$ = 5700 y) and ^{37}Ar ($T_{1/2}$ = 35 d). Air leakage control and pressurization need to be defined to prevent the activated air from contaminating the room adjacent to the TC.

3.3. Neutronics activities in lithium systems

The main functions of the lithium systems (LS) are to provide a 25 mm thick and 260 mm wide stable lithium target to fully stop 40 MeV deuteron beams, remove the 5 MW deposited power, and produce neutrons through d-Li reactions. The target assembly (TA) provides a concave channel for the 25 mm thick Li jet which flows in a high speed of 15 m/s. The concave channel builds a free surface for the incident deuteron beam, and increases the Li pressure by centrifugal force to avoid boiling and significant evaporation. As shown in Fig. 13, the LS consists of a triple heat exchanger system with a lithium-oil loop, an oil-oil loop, and an oil-water loop. It is worth mentioning that the Impurity Control System (ICS) is an important part of the LS. The ICS is designed to remove the radioisotopes ^{7}Be and ACP with Cold Traps (CT), remove ^{3}H with hydrogen traps (H-Trap), and remove other impurities through chemical traps.

^{7}Be ($T_{1/2}$ = 53.2 d) is produced mainly in the d-Li interaction through the reactions ^{6}Li(d,n)^{7}Be (15 %) and ^{7}Li(d,2n)^{7}Be (83 %) [46] and emits 477 keV gammas in 10.4 % of its decay. The production rate of ^{7}Be is 0.75 g/fpy (9.7 × 10^{15} Bq/fpy) [47], which reaches an equilibrium inventory of 0.15 g (2.0 × 10^{15} Bq) after 1 fpy of DONES operation without purifications. The total ^{3}H production rate is ~3.78 g/fpy (1.35 × 10^{15} Bq/fpy, 80 % from d-Li reactions and 20 % from n-Li reactions),
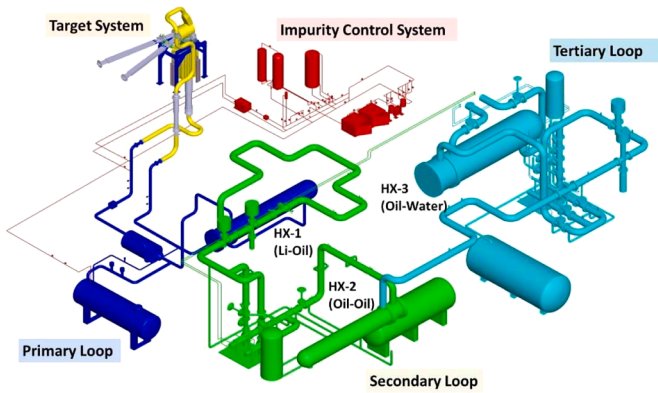
Fig. 13. schematic view of the lithium system.

which is similar to half of the IFMIF value in Ref. [47]. Note that the nuclear data for deuteron-induced [7]Be and ^{3}H production still have high uncertainties [48], which will be discussed in the later sections.

[7]Be has a significant impact on radiation safety, and its distribution in the lithium loop in the form of Be_3N_2 varies with the operating temperature T_{Li}, mass flow rate Q_{CT} of the CT, and trap efficiency η. Under the previous baseline conditions of $T_{Li} = 250$ °C, $\eta = 60$ %, and $Q_{CT} = 0.5$ %, the radiation in the lithium loop cell (LLC) is shown in Fig. 14, where several Sv/h of high doses are imposed in the LLC. To concentrate most of the [7]Be in the CT, the lithium operating condition is increased to $T_{Li} = 300$ °C, $\eta = 75$ %, and $Q_{CT} = 2$ % [1], thus significantly reducing the radiation from [7]Be in the LLC.

ACPs are another critical radiation source, which consists of a list of radioisotopes produced by deuteron and neutron activation of corrosion products from EUROFER and SS316L. These radioisotopes include, but are not limited to, [28]Al ($T_{1/2} = 134$ s), [52]V ($T_{1/2} = 255$ s), [56]Mn ($T_{1/2} = 2.57$ h), [54]Mn ($T_{1/2} = 312$ d), [56]Co ($T_{1/2} = 77$ d), [57]Co ($T_{1/2} = 272$ d), [60]Co ($T_{1/2} = 5.27$ y), [55]Fe ($T_{1/2} = 2.75$ y), all of which are strong gamma emitters except [57]Co and [55]Fe. Simulations of ACP are performed using
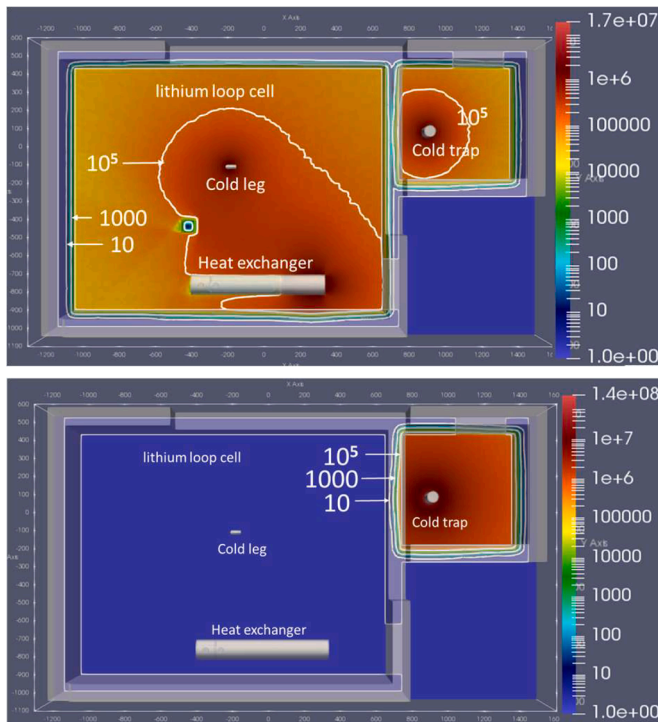
mass transfer studies of the lithium loop. These simulations consider the production rates computed in different sections of the loop, as well as the solubilities and mass transfer coefficients under different temperature conditions. The simulations are still ongoing, and there are many challenges associated with simulating ACP, and their impact on the radiation levels in the lithium rooms.

In addition to [7]Be and ACP, radiation also comes directly from TC during operation. However, the dose level as shown in Fig. 15 is not significantly high. The dose rate during operation in the Test Cell - Lithium System Interface Cell (TLIC), a forbidden-access area, is at the level of 100 mSv/h with a hotspot of 1 Sv/h at the outlet. The TLIC structure further attenuates the dose rate to < 10 mSv/h outside the TLIC. The low neutron fluxes outside the TLIC will not induce a significant amount of activation on the argon atmosphere and structure.

3.4. Neutronics activities in other systems and areas

Beam-on and beam-off radiations and component activations have important implications for safety [49], remote handling and logistics, Radioactive Waste Treatment Systems (RWTS), Building and Plant Systems (BPS), etc. For example, as shown in Fig. 16, the shutdown dose during maintenance requires the computation of the gamma doses of the highly activated HFTM transported from the opened TC. This results in biological dose rates of 10–100 Sv/h near the HFTM and 1–10 Sv/h from the opened TC. The gamma doses result in high absorbed doses to the electronics, radiation to neighboring rooms, and potentially sky-shine to the public. To confirm the wall thickness of the RWTS rooms, decay gammas shielding calculations have been further performed using the irradiated HFTM module, as well as other irradiated modules such as TA and HEBT scrapers, transported in these rooms (e.g., R-157 in Fig. 17). The results suggest increasing the wall of several solid RWTS rooms from 1.0 m thick to 1.5 m thick to reduce the doses to <10 μSv/h required for the adjacent rooms. The residual doses of HFTM are dominated by [58]Co ($T_{1/2} = 70.9$ d) and [54]Mn ($T_{1/2} = 312$ d), which have relatively long half-lives, thus the residual doses remain rather strong from one day to one year. Besides the solid RW, the liquid RW has also been assessed based on several source terms from activated Li, cooling water, oil, etc. Fig. 18 shows that the residual doses from the 7.33 mg [7]Be in 27 m[3] of Li (a conservative assumption) can be shielded by the current wall thickness. The results are subject to be re-evaluated once the ACP data is updated.

In addition to material irradiations, DONES provides the possibility to conduct experiments on nuclear physics, medical physics, and other applications in the Complementary Experimental Room (CER) next to the TC on the beam downstream. A neutron beam tube with $R = 100$ mm provides a neutron flux of up to 1×10^{10} n/cm[2]/s at the exit of the rotating disk shutter. Although this tube is relatively small, the neutron dose rate in the CER reaches above 100 mSv/h when the shutter is opened, as shown in Fig. 19. The 1 m thick shielding wall is not able to reduce the doses below the limit of 10 mSv/h, nor reduce the dose to the public to the level of < 0.5 mSv/h. An additional increase of 0.5 m thick

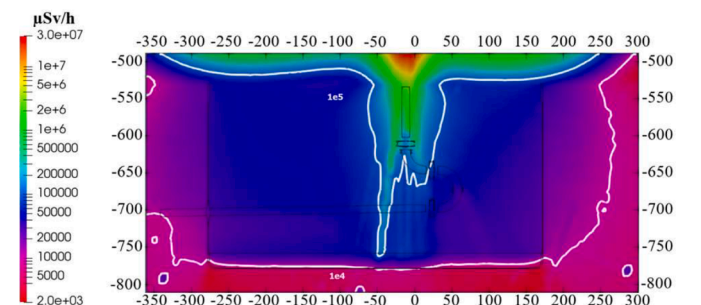**Fig. 14.** Radiation dose map (μSv/h) contributed by [7]Be during operation. Top – under operation temperature of 250 °C, and bottom – under 300 °C.

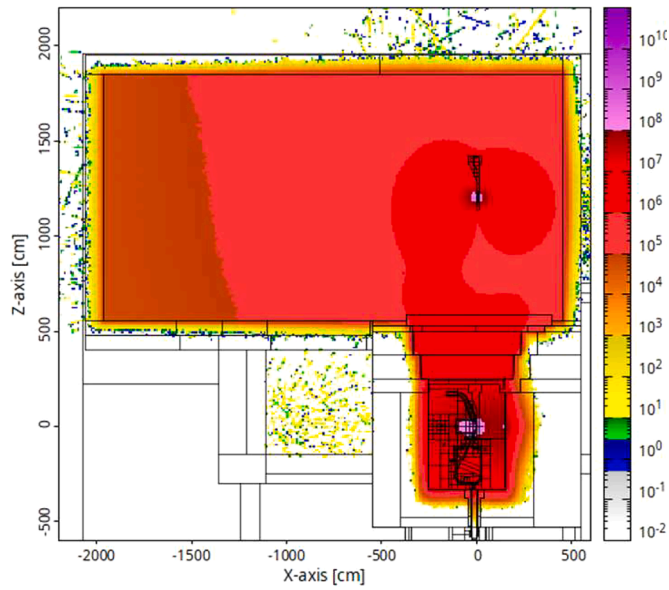**Fig. 15.** The total neutron and gamma doses (μSv/h) contributed from the TC to the LLC.

Fig. 16. Shutdown dose rate (μSv/h) during TC opened and HFTM transportation after 345 days of operation and 1-day cooling.
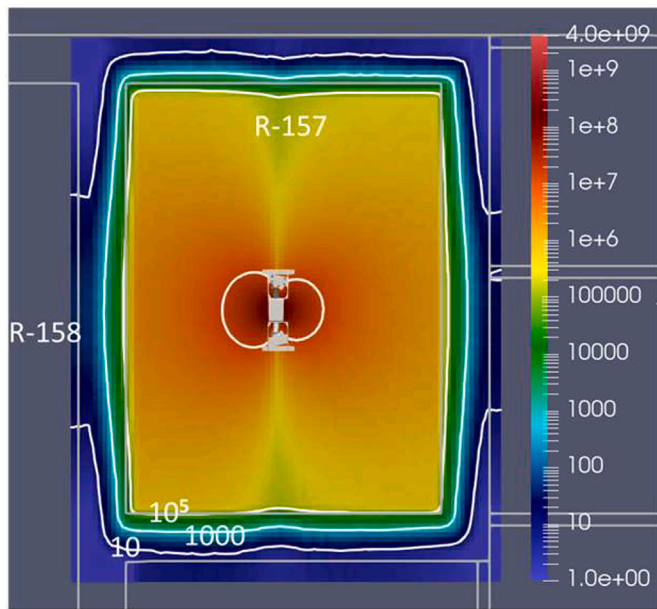

Fig. 18. The biological dose rate (μSv/h) induced by 7.33 mg of ^{7}Be in the liquid waste storage cell.

Fig. 17. Shutdown dose rate (μSv/h) in the RWTS room R157 contributed by HFTM after 1-day cooling.
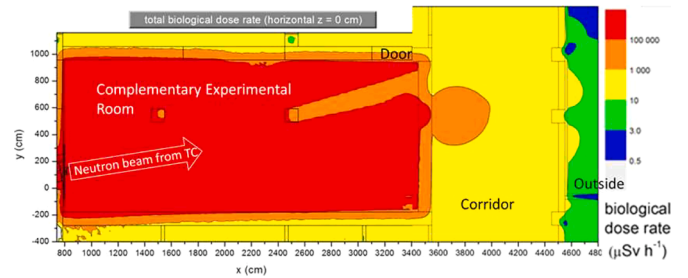
Fig. 19. Neutron dose rate (μSv/h) during operation and shutter opened in the CER.
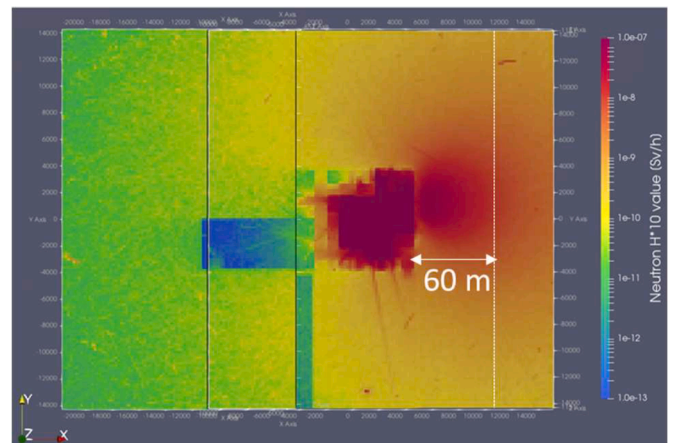
Fig. 20. Neutron dose rate (Sv/h) at the ground level contributed from direct radiation exposure and sky-shine during operation.

concrete on the wall is planned to be implemented, along with additional polyethylene slabs for the radiation leakage through the ventilation penetrations. The potential impact of this shielding weakness on the direct exposure and skyshine analysis is shown in Fig. 20. It can be observed from this map that the value is 0.01–0.05 μSv/h at a distance of 60 m away from the building, which is very likely due to the shielding weakness in the CER. Further assessment will be provided as the CER shieldings are currently improved.

4. Nuclear data, experiments and other activities

4.1. Nuclear data

Recent developments in deuteron data evaluations have strong implications for nuclear simulations for the DONES project. The release of
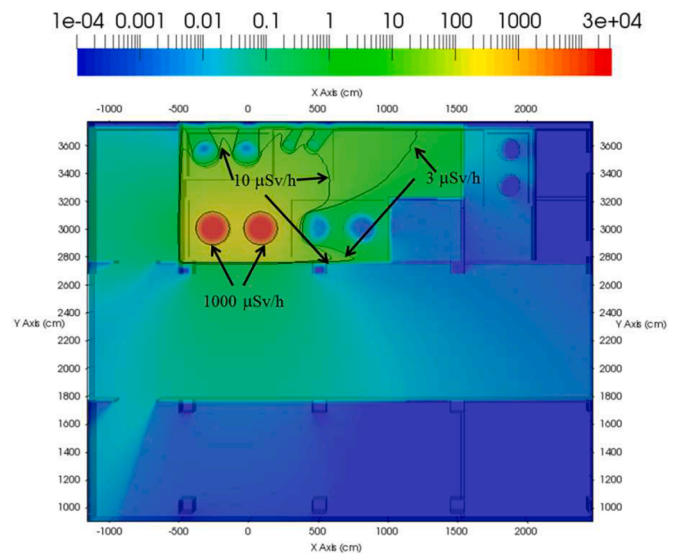
the JENDL/DEU-2020 data provides alternative d-Li evaluations for comparison with the current reference FZK-2005 evaluations [7]. A comparison in Ref. [8] reveals discrepancies between the FZK-2005 and JENDL/EU-2020 data in terms of neutron yield. FZK-2005 shows better agreement with the experimental data for the 0° neutron emissions on the broad 14 MeV peak produced from d-Li stripping reactions, but relatively higher estimations on the 1 MeV peak, which are neutrons

produced isotropically from the evaporation process [50]. In the center 16 capsules, deviations in neutron flux and damage dose rate are up to 10 %−20 %, but in the lateral capsules, deviations are as high as 30–40 %. Since the material samples are located in the center capsules, and the displacement cross sections in 14 MeV are higher than in 1 MeV, the d-Li data for the stripping reactions plays a key role. Although the analysis in Ref. [8] suggests that the JENDL/EU-2020 data is more reliable, additional experimental data is needed in the forward angle. In addition to d-Li data, a comparison in Ref. [32] also provides evidence that the JENDL-5 data has better agreement with the experimental data of d-Cu data (Fig. 21), even with the improved accuracy from the breakup kinematics described in Ref. [51].

In addition to the uncertainty in d-Li neutron yields, there is also significant uncertainty in the activation data for ^{7}Be and ^{3}H production. A study [48] found large discrepancies between the FZK-2005 and TENDL-2017 evaluations of the ^{6,7}Li(d,x)^{3}H reaction, as well as some deficiencies in both evaluations of the ^{6,7}Li(d,x)^{7}Be reaction. Unfortunately, the JENDL-5 deuteron data does not provide activation data for these two isotopes. This has been identified as a high-priority need by the nuclear community and has been submitted to the IAEA nuclear data High Priority Request List (HPRL), with contributions being received recently, such as experiments with low-energy deuteron [52].

4.2. Neutronics experiments

One important ongoing activity is the DONES shielding mock-up experiments, which aim to characterize the shielding performance of ordinary concrete and heavy concrete in the DONES TC environment. The facility selected for this experiment is the neutron source in the NPI Řež cyclotron U120M, which accelerates a proton beam to 35 MeV impinging on Be target, producing a continuous neutron spectrum up to 33 MeV [53]. The ordinary and heavy concrete mock-ups were supplied and designed by WUT and UGR Team based on ITER concrete classes C40/50, but using local cement and limestone aggregate from the Granada site, and imported magnetite heavy aggregates. Due to material and composition optimization, the mechanical properties of samples have been much higher than the reference ITER concrete – after 90 days of curing it was obtained almost 80 MPa of compressive strength and about 10 MPa of flexural strength [54]. The slabs produced have dimensions of $50 \times 50 \times 5$ cm^3, and densities of 2.5 g/cm^3 for ordinary concrete and 3.9 g/cm^3 for heavy concrete, as estimated in the predesign stage. A mock-up with dimensions of $70 \times 70 \times 100$ cm^3 was proposed, Fig. 22, by adding additional slabs surrounding the center blocks to reduce neutron leakage and room scattering effects. Activation foils of Fe, Al, Ti, Au and In were installed throughout the full depths of the mock-ups to capture neutron fluxes and spectra at different locations. Five locations were used in the ordinary concrete experiment: 0 cm, 25 cm, 50 cm, 75 cm and 100 cm. Eight locations were used for the heavy concrete: 0 cm, 25 cm, 35 cm, 45 cm, 55 cm, 65 cm, 75 cm and 90 cm.
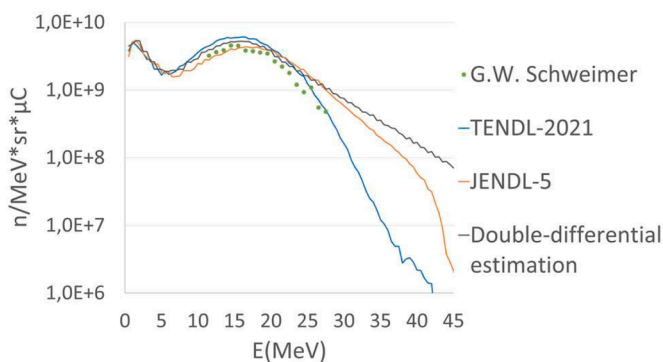

Fig. 21. Neutron yield at 0° from d-Cu nuclear data at the deuteron energy of 40 MeV.
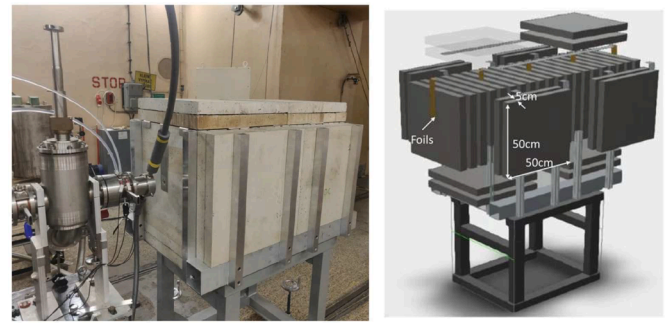

Fig. 22. Shielding mockup design (right) and experiment setup(left).

Experiments were recently completed with good statistics obtained for the foils installed for both ordinary and heavy concrete. Follow-up post-irradiation analysis is ongoing. The activity will continue with the measurement of the chemical compositions and bounded hydrogen contents so that the neutron shielding performance of the candidate concrete can be characterized for the construction of DONES.

Experiments at the Linear IFMIF Prototype Accelerator (LIPAc) under the European and Japanese collaboration framework Broader Approach phase II (BA-II) are also useful in many ways. LIPAc commissioning under 125 mA deuterium beam at 5 MeV and 9 MeV Continuous Wave (CW) conditions will produce a source of neutrons with energies higher than 4 MeV of up to 3×10^{13} s^{-1} through the d-Cu interaction at the Beam Dump (BD). The measurements performed during the LIPAc commissioning phase will provide reference data for radiation assessment of the DONES commissioning phases 1 and 2, and nuclear diagnostics behavior under DONES-like conditions. In addition, those neutrons can be used to activate candidate materials for the DONES accelerators and to validate neutron transport tools (e.g., MCUNED, D1SUNED, MCNP6) and data (e.g., TENDL, JENDL, FENDL) for beam-on and beam-off particle transport, activation, and shutdown dose assessment. These data are essential for the licensing of the DONES commissioning, as well as useful for both EU [55] and Japan with the synergies of building fusion neutron sources.

Since neutronics are transversal activities, the data and reports produced are valuable for design evolution over time. One document to facilitate data referencing is the Nuclear Analysis Handbook (NAH), which summarizes the essential outcomes of most relevant analyses on e.g. neutronics models, fluxes and spectra, nuclear heating, radiation source terms, radiation dose maps and absorbed dose maps, activation inventory data categorized by the systems in the Work Breakdown Structure (WBS), as well as material definitions and neutronics guidelines for the consistencies of nuclear analyses. It provides a central document guiding the user in the project to the available and up-to-date data, as well as references to the underlying reports and publications. The NAH is updated annually to include the latest results.

It is worth mentioning that two databases for activated components have been established. An activation inventory database provides tables and graphs of total and specific activities, contact doses, decay heat, dominant isotopes, etc. for highly activated components such as the HFTM, TA, HEBT scraper, beam dump, liner, and RBSB. The database currently provides data for TC components produced automatically using the FISPACT-II API feature. Another database focuses on collecting available decay gamma sources on these activated components, which is beneficial for future simulations on transporting radioactive waste and avoiding unnecessary repetition of tedious and resource-intensive Rigorous 2-step (R2S) shutdown dose calculations. These activities efficiently provide high-quality input for performing analyses upon urgent needs.

5. Summary and outlook

5.1. Summary

The neutronics activities in the EUROfusion work package ENS have made significant progress in the past few years of framework program FP9, with joint efforts from multiple EU research units. The AS nuclear analyses cover both the commissioning phases and normal operation phase, assessing the radiation from major sources such as deuteron beam losses, critical beam deposition locations of MEBT and HEBT scrapers, beam dumps, TC neutrons, and the consequent water and atmosphere activations. The TS nuclear analyses answer key questions on the material irradiation performance of the facility, and the shielding optimizations to reduce the radiation impact on the surrounding rooms. The analysis on LS characterizes the critical source terms ^{7}Be, ^{3}H, and ACP, and the radiation impacts on the lithium rooms. The analysis of other systems obtains the inventory and residual doses comprising highly activated solid waste (e.g., HFTM), liquid waste (e.g. ^{7}Be), shielding of the CER, as well as direct exposure and skyshine to the public area during operation.

Tools, methods, and data for particle transport, activation, residual doses, and radiation shielding have been continuously improved in the past decade. For deuteron data, several evaluation activities are ongoing for d-Li, d-Cu, and other data most relevant to accelerator systems. The shortcomings in the deuteron data will be addressed with high priority in the future. Shielding mock-up experiments have been manufactured and tested with a high-energy neutron source, using ordinary and heavy concrete that are relevant to the future construction of DONES. A highlight of the EU-Japan collaboration under BA-II is the use of LIPAc facilities for material activation and code validations, which benefits from the synergies of building a neutron source for fusion material irradiation. The NAH, the activation inventory database, and the decay gamma source database are the recent activities to provide efficiently high-quality data for the overall project.

5.2. Outlook

Several challenges remain despite the progress in DONES neutronics. d-Li data, in particular, are essential and has a direct impact on the qualification of irradiation performance and safety assessment. This is currently being addressed through collaborations within EU, such as the nuclear data community's contribution to the HPRL and the EU-Japan bilateral agreement on the validation of JENDL5 data. To determine the damage doses received by the samples, one ongoing work is to assess the overall uncertainties from beam dynamics, geometry modeling, d-Li data, and displacement cross section. Another important activity to achieve high spatial DPA measurement is the implementation and data retrieval of online and offline detectors, in which methodologies and technologies have to be further developed. In addition, nuclear analyses must be continuously updated to resolve existing radiation protection issues, such as the shielding weakness in the CER, public doses from other radiation source terms, residual doses from the ACP in Li, water activation, etc. More importantly, the tools and data need to be further validated and verified under conditions similar to the ones in DONES to ensure the quality of the results and the successful licensing of the facility for commissioning and operation.

CRediT authorship contribution statement

Y. Qiu: Formal analysis, Methodology, Software, Visualization, Writing – original draft. **M. Ansorge:** Formal analysis, Methodology, Software, Validation, Writing – review & editing. **I. Álvarez:** Formal analysis, Methodology, Software, Visualization, Writing – review & editing. **K. Ambrožič:** Formal analysis, Methodology, Software, Visualization, Writing – review & editing. **T. Berry:** Formal analysis, Methodology, Software, Writing – review & editing. **B. Bieńkowska:** Formal analysis, Methodology, Software, Visualization, Writing – review & editing. **H. Chohan:** Formal analysis, Methodology, Software, Visualization, Writing – review & editing. **A. Čufar:** Formal analysis, Methodology, Software, Visualization, Writing – review & editing. **D. Dworak:** Formal analysis, Methodology, Software, Visualization, Writing – review & editing. **T. Dezsi:** Formal analysis, Methodology, Software, Visualization, Writing – review & editing. **T. Eade:** Formal analysis, Methodology, Software, Visualization, Writing – review & editing. **J. García:** Formal analysis, Methodology, Software, Visualization, Writing – review & editing. **D. Jimenez-Rey:** Formal analysis, Investigation, Software, Visualization, Writing – review & editing. **I. Lengar:** Methodology, Writing – review & editing. **A.J. Lopez-Revelles:** Formal analysis, Methodology, Software, Visualization, Writing – review & editing. **V. Lopez:** Formal analysis, Methodology, Software, Visualization, Writing – review & editing. **E. Mendoza:** Formal analysis, Methodology, Software, Visualization, Writing – review & editing. **F. Mota:** Formal analysis, Methodology, Software, Validation, Writing – review & editing. **M.J. Martinez-Echevarria:** Formal analysis, Methodology, Software, Visualization, Writing – review & editing. **F. Ogando:** Formal analysis, Methodology, Software, Visualization, Writing – review & editing. **J. Park:** Formal analysis, Methodology, Software, Visualization, Writing – review & editing. **T. Piotrowski:** Formal analysis, Methodology, Software, Visualization, Writing – review & editing. **A. Serikov:** Formal analysis, Methodology, Software, Visualization, Writing – review & editing. **G. Stankunas:** Formal analysis, Methodology, Software, Visualization, Writing – review & editing. **A. Tidikas:** Formal analysis, Methodology, Software, Visualization, Writing – review & editing. **G. Tracz:** Formal analysis, Methodology, Software, Visualization, Writing – review & editing. **G. Žerovnik:** Formal analysis, Methodology, Software, Visualization, Writing – review & editing. **F. Arbeiter:** Methodology, Validation, Writing – review & editing. **F. Arranz:** Validation, Writing – review & editing. **S. Becerril:** Validation, Writing – review & editing. **P. Cara:** Validation, Writing – review & editing. **D. Bernardi:** Validation, Writing – review & editing. **J. Castellanos:** Validation, Writing – review & editing. **J. Gutiérrez:** Validation, Writing – review & editing. **A. Ibarra:** Project administration, Writing – review & editing. **W. Królas:** Project administration, Writing – review & editing. **J. Maestre:** Validation, Writing – review & editing. **F. Martín-Fuertes:** Validation, Writing – review & editing. **J.C. Marugán:** Validation, Writing – review & editing. **G. Micciché:** Validation, Writing – review & editing. **J. Martínez-Serrano:** Formal analysis, Methodology, Software, Validation, Writing – review & editing. **F.S. Nitti:** Validation, Writing – review & editing. **I. Podadera:** Validation, Writing – review & editing. **U. Wiącek:** Validation, Writing – review & editing. **U. Fischer:** Validation, Writing – review & editing.

Declaration of competing interest

The authors declare that they have no known competing financial interests or personal relationships that could have appeared to influence the work reported in this paper.

Data availability

Data will be made available on request.

Acknowledgments

References

[1] W. Królas, et al., The IFMIF-DONES fusion oriented neutron source: evolution of the design, Nucl. Fusion 61 (12) (2021) 125002, https://doi.org/10.1088/1741-4326/ac318f.

[2] A. Ibarra, et al., The European approach to the fusion-like neutron source: the IFMIF-DONES project, Nucl. Fusion 59 (6) (2019) 065002, https://doi.org/10.1088/1741-4326/ab0d57. Jun.

[3] A. Maj, M.N. Harakeh, M. Lewitowicz, A. Ibarra, W. Krolas, 2016 White Book on the complementary scientific pro- gramme at IFMIF-DONES, IFJ-PAN Rep. 2094/PL (2016) [Online]. Available: https://ifj.edu.pl/badania/publikacje/raporty/2016/2094.pdf.

[4] P. Sauvan, J. Sanz, F. Ogando, New capabilities for Monte Carlo simulation of deuteron transport and secondary products generation, Nucl. Instrum. Methods Phys. Res. Sect. A Accel. Spectromet Detect. Assoc. Equip. 614 (3) (2010) 323–330, https://doi.org/10.1016/j.nima.2009.12.084.

[5] S.P. Simakov, U. Fischer, K. Kondo, P. Pereslavtsev, Status of the McDeLicious approach for the D-Li neutron source term modeling in ifmif neutronics calculations, Fusion Sci. Technol. 62 (1) (2012) 233–239.

[6] C.J. Werner, MCNP users manual-code version 6.2, Los Alamos Natl. Lab. 746 (2017).

[7] P. Pereslavtsev, U. Fischer, S. Simakov, M. Avrigeanu, Evaluation of d +6,7Li data for deuteron incident energies up to 50 MeV, Nucl. Instrum. Methods Phys. Res. Sect. B Beam Interact. with Mater. Atoms (2008), https://doi.org/10.1016/j.nimb.2008.05.014.

[8] E. Mendoza, et al., Nuclear data libraries for IFMIF-DONES neutronic calculations, Nucl. Fusion 62 (10) (2022), https://doi.org/10.1088/1741-4326/ac814f.

[9] O. Iwamoto, et al., Japanese evaluated nuclear data library version 5: JENDL-5, J. Nucl. Sci. Technol. 60 (1) (2023) 1–60, https://doi.org/10.1080/00223131.2022.2141903.

[10] F. Ogando, Advanced Monte-Carlo method for prompt and residual radiation calculations in light-ion accelerators, in: Proceedings of the SATIF-15, 2022.

[11] Y. Hu, Y. Qiu, U. Fischer, Extension and benchmarking of the OpenMC code for accelerator-based neutron source applications, Fusion Eng. Des. 161 (2020), https://doi.org/10.1016/j.fusengdes.2020.112059.

[12] L. Lu, Y. Qiu, U. Fischer, Improved parallel solid decomposition algorithms for the CAD-to-MC conversion tool McCad, Fusion Eng. Des. 124 (2016) 1269–1272, https://doi.org/10.1016/j.fusengdes.2017.02.040.

[13] Y. Wu, et al., CAD-based Monte Carlo program for integrated simulation of nuclear system SuperMC, Ann. Nucl. Energy 82 (2015) 161–168.

[14] A. Travleev, "Numjuggler," 2016. https://github.com/inr-kit/numjuggler.

[15] J.P. Catalán, P. Sauvan, J. García, J. Alguacil, F. Ogando, J. Sanz, GEOUNED: a new conversion tool from CAD to Monte Carlo geometry, Nucl. Eng. Technol. (2024), https://doi.org/10.1016/j.net.2024.01.052 no. In Press.

[16] J.-C. Sublet, J.W. Eastwood, J.G. Morgan, M.R. Gilbert, M. Fleming, W. Arter, FISPACT-II: an advanced simulation system for activation, transmutation and material modelling, Nucl. Data Sheets 139 (2017) 77–137.

[17] J. Sanz, O. Cabellos, and N. García-Herranz, "ACAB Inventory code for nuclear applications: user's manual V. 2008," NEA-1839, vol. 6, pp. 475–480, 2008.

[18] G. Bailey, D. Foster, P. Kanth, and M. Gilbert, "The FISPACT-II user manual," Culham Cent. Fusion Energy (CCFE), Culham, UK, Tech. Rep. UKAEA-CCFE-RE, vol. 2, 2021.

[19] T. Eade, B. Colling, J. Naish, L.W. Packer, A. Valentine, Shutdown dose rate benchmarking using modern particle transport codes, Nucl. Fusion 60 (5) (2020), https://doi.org/10.1088/1741-4326/ab8181.

[20] A. Travleev, "R2Smesh-at: implementation of R2S method for SDDR," 2020. https://github.com/travleev/r2smesh-at.

[21] P. Sauvan, J.P. Catalán, F. Ogando, R. Juárez, J. Sanz, Development of the R2SUNED code system for shutdown dose rate calculations, IEEE Trans. Nucl. Sci. 63 (1) (2016) 375–384.

[22] V. Lopez, P. Sauvan, F. Ogando, Shutdown dose rates calculations due to light ions induced activation using D1S methodology, Fusion Eng. Des. 167 (January) (2021) 112298, https://doi.org/10.1016/j.fusengdes.2021.112298.

[23] T.A. Berry, et al., Integration of fluid dynamics into activation calculations for fusion, Fusion Eng. Des. 173 (2021) 112894, https://doi.org/10.1016/j.fusengdes.2021.112894.

[24] J. García, Y. Qiu, C. Torregrosa, Development of radiation sources based on CAD models for the nuclear analysis of IFMIF-DONES lithium loop, Fusion Eng. Des. (2024) (under review).

[25] S.W. Mosher, et al., ADVANTG: An Automated Variance Reduction Parameter Generator, 2015.

[26] Y. Zheng, Y. Qiu, P. Lu, Y. Chen, U. Fischer, S. Liu, Improvements of the on-the-fly MC variance reduction technique with dynamic WW upper bounds, Nucl. Fusion 62 (8) (2022), https://doi.org/10.1088/1741-4326/ac75fc.

[27] A.J. Koning, D. Rochman, J.C. Sublet, N. Dzysiuk, M. Fleming, S. van der Marck, TENDL: complete nuclear data library for innovative nuclear science and technology, Nucl. Data Sheets 155 (2019) 1–55, https://doi.org/10.1016/j.nds.2019.01.002.

[28] A.J. Koning, M.C. Duijvestijn, and S. Hilaire, TALYS-1.0. France: EDP sciences, 2008. [Online]. Available: http://inis.iaea.org/search/search.aspx?orig_q=RN:41034220.

[29] U. Fischer, et al., Nuclear data activities of the EUROfusion consortium, EPJ Web Conf. 239 (2020) 21001, https://doi.org/10.1051/epjconf/202023921001.

[30] M. Avrigeanu, et al., Advanced breakup-nucleon enhancement of deuteron-induced reaction cross sections, Eur. Phys. J. A 58 (1) (2022) 1–13, https://doi.org/10.1140/epja/s10050-021-00659-6.

[31] S. Nakayama, O. Iwamoto, Y. Watanabe, K. Ogata, JENDL/DEU-2020: deuteron nuclear data library for design studies of accelerator-based neutron sources, J. Nucl. Sci. Technol. 58 (7) (2021) 805–821, https://doi.org/10.1080/00223131.2020.1870010.

[32] V. Lopez, F. Ogando, P. Sauvan, Sensitivity to nuclear data of the design of the IFMIF-DONES beam dump, Front. Phys. 11 (2023) [Online]. Available: https://www.frontiersin.org/articles/10.3389/fphy.2023.1144057.

[33] "FENDL-3.1d: fusion evaluated nuclear data library Ver.3.1d" https://www-nds.iaea.org/fendl31d/.

[34] G. Schnabel, et al., FENDL : a library for fusion research and applications, Nucl. Data Sheets 193 (2024) 1–78.

[35] A.Y. Konobeyev, U. Fischer, P.E. Pereslavtsev, Evaluation of advanced displacement crosssections for the major EUROFER constituents based on an atomistic modelling approach, Kerntechnik 80 (1) (2015) 7–12, https://doi.org/10.3139/124.110483/MACHINEREADABLECITATION/RIS. Mar.

[36] I. Podadera, et al., The accelerator system of Ifmif-Dones multi-Mw facility, in: Proceedings of the IPAC2021, 2021, pp. 2–5, https://doi.org/10.18429/JACoW-IPAC2021-TUPAB211.

[37] F. Ogando, L. Macia, V. Lopez, I. Podadera, D. Sanchez-Herranz, Beam-facing material selection for mitigation of residual doses in the HEBT of IFMIF-DONES, Nucl. Mater. Energy 38 (2024) 101592, https://doi.org/10.1016/j.nme.2024.101592.

[38] I. Podadera, et al., Commissioning plan of the IFMIFDONES accelerator, in: Proceedings of the LINAC'22, 2022.

[39] K. Kondo, et al., Neutron production and dose rate in the IFMIF/EVEDA LIPAc injector beam commissioning, Fusion Eng. Des. 109–111 (2016) 1104–1108, https://doi.org/10.1016/j.fusengdes.2016.01.014.

[40] T. Berry, et al., Recent nuclear analysis of the IFMIF-DONES phase 2 commissioning accelerator and MEBT, in: Proceeding of the IEEE Symposium on Fusion Engineering (SOFE), 2023.

[41] V. Belous, G. Kalinin, P. Lorenzetto, S. Velikopolskiy, Assessment of the corrosion behaviour of structural materials in the water coolant of ITER, J. Nucl. Mater. 258–263 (1998) 351–356, https://doi.org/10.1016/S0022-3115(98)00272-4.

[42] B. Van der Schaaf, et al., The development of EUROFER reduced activation steel, Fusion Eng. Des. 69 (1–4) (2003) 197–203, https://doi.org/10.1016/S0920-3796(03)00337-5. Sep.

[43] D. Bernardi, et al., The IFMIF-DONES project: design status and main achievements within the EUROfusion FP8 work programme, J. Fusion Energy 41 (2) (2022) 1–26, https://doi.org/10.1007/s10894-022-00337-5.

[44] Y. Qiu, F. Arbeiter, U. Fischer, K. Tian, Neutronics analyses for the bio-shield and liners of the IFMIF-DONES test cell, Fusion Eng. Des. 146 (2019) 723–727, https://doi.org/10.1016/j.fusengdes.2019.01.064.

[45] Y. Qiu, et al., Potential use of IFMIF-DONES target back-plate for material specimens, J. Nucl. Eng. 3 (4) (2022) 385–397.

[46] M. Frisoni, D. Bernardi, F.S. Nitti, Nuclear assessment of the IFMIF-DONES lithium target system, Fusion Eng. Des. 157 (March) (2020) 111658, https://doi.org/10.1016/j.fusengdes.2020.111658.

[47] S.P. Simakov, U. Fischer, U. Von Möllendorff, Assessment of the 3H and 7Be generation in the IFMIF lithium loop, J. Nuclear Mater. (2004) 213–217, https://doi.org/10.1016/j.jnucmat.2004.04.024.

[48] S.P. Simakov, U. Fischer, and A.Y. Konobeyev, "Status and benchmarking of the deuteron induced Tritium and Beryllium-7 production cross sections in Lithium," KIT Sci. Work. Pap., no. 147, 2020. 10.5445/IR/1000102615.

[49] F. Martín-Fuertes, et al., Implementation of safety aspects in IFMIF-DONES design, J. Nucl. Eng. 3 (4) (2022) 373–384.

[50] M. Ohta, S. Kwon, S. Sato, K. Ochiai, H. Suzuki, Analysis of radionuclidic purity of medical isotope production with d-Li neutron in A-FNS, Fusion Eng. Des. 146 (December 2018) (2019) 207–211, https://doi.org/10.1016/j.fusengdes.2018.12.019.

[51] P. Sauvan, A. Koning, F. Ogando, J. Sanz, Implementation of a new energy-angular distribution of particles emitted by deuteron induced nuclear reaction in transport simulations, EPJ Web Conf. (2017), https://doi.org/10.1051/epjconf/201714602010.

[52] D. Koliadko, et al., High priority request list cross-section measurements : 7 Li (d, x) 7 Be /3 H and K (n, p) 39 Ar, EPJ Web Conf. 284 (2023), https://doi.org/10.1051/epjconf/202328401026. Volume.

[53] M. Majerle, et al., Measurements of the neutron spectra from the p+Be neutron generator of the NPI CAS, Nucl. Instrum. Methods Phys. Res. Sect. A Accel. Spectrom. Detect. Assoc. Equip. 1053 (December 2022) (2023) 168314, https://doi.org/10.1016/j.nima.2023.168314.

[54] T. Piotrowski, et al., Optimization and evaluation of structural and shielding concrete for IFMIF-DONES, Nucl. Mater. Energy (2024) 101597, https://doi.org/10.1016/j.nme.2024.101597 vol. In Press.

[55] D. Jimenez, Overview of European fusion neutron source activities within the IFMIF/EVEDA project, in: Proceedings of the 15th International Symposium on Fusion Nuclear Technology (ISFNT-15), 2023.